Cell Metabolism
Article

An SREBP-Responsive microRNA Operon Contributes to a Regulatory Loop for Intracellular Lipid Homeostasis

Tae-Il Jeon,[1,3,6] Ryan M. Esquejo,[1,6] Manuel Roqueta-Rivera,[1] Peter E. Phelan,[1] Young-Ah Moon,[4] Subramaniam S. Govindarajan,[2] Christine C. Esau,[5] and Timothy F. Osborne[1,*]
[1]Metabolic Signaling and Disease Program and Diabetes and Obesity Center
[2]Analytical Genomics Core Facility
Sanford-Burnham Medical Research Institute, Orlando, Florida 32827, USA
[3]Department of Animal Science, College of Agriculture & Life Science, Chonnam National University, Gwanju 500-757, South Korea
[4]Department of Molecular Genetics, University of Texas Southwestern Medical Center, Dallas, Texas 75235, USA
[5]Regulus Therapeutics, San Diego, California 92121, USA
[6]These authors contributed equally to this work
*Correspondence: tosborne@sanfordburnham.org
http://dx.doi.org/10.1016/j.cmet.2013.06.010

SUMMARY

Sterol regulatory element-binding proteins (SREBPs) have evolved as a focal point for linking lipid synthesis with other pathways that regulate cell growth and survival. Here, we have uncovered a polycistronic microRNA (miRNA) locus that is activated directly by SREBP-2. Two of the encoded miRNAs, miR-182 and miR-96, negatively regulate the expression of Fbxw7 and Insig-2, respectively, and both are known to negatively affect nuclear SREBP accumulation. Direct manipulation of this miRNA pathway alters nuclear SREBP levels and endogenous lipid synthesis. Thus, we have uncovered a mechanism for the regulation of intracellular lipid metabolism mediated by the concerted action of a pair of miRNAs that are expressed from the same SREBP-2-regulated miRNA locus, and each targets a different protein of the multistep pathway that regulates SREBP function. These studies reveal an miRNA "operon" analogous to the classic model for genetic control in bacterial regulatory systems.

INTRODUCTION

Sterols and fatty acids are the two major lipid classes in mammalian cells, and both are critical membrane components that are continuously required for maintaining cell integrity and supporting optimal growth. These lipids are also utilized for more specialized roles that rely on their unique physical properties to influence diverse biological processes. Over the last several decades, major advances in understanding the regulation of lipid metabolism that have been fueled by parallel advances in cell, molecular, and genomic sciences have occurred, and these advances continue to revolutionize biomedical research. The pioneering studies from Brown and Goldstein (2009) have provided many of the elegant advances in cell cholesterol (Ch) regulation, including the discovery of a pathway for Ch uptake through the low-density lipoprotein (LDL) receptor, which is regulated in balance with an endogenous Ch production pathway centered on two endoplasmic reticulum (ER) membrane proteins, HMG CoA reductase and sterol regulatory element-binding proteins (SREBPs).

Mammalian SREBPs regulate the genes of both Ch and fatty acid metabolism, and recent studies have shown that they link lipid metabolism to cell growth and survival through the direct activation of additional key target genes of other cellular processes (Jeon and Osborne, 2012). Synthesized as ~125 KDa precursors, SREBPs are composed of an amino-terminal transcription factor domain connected to a membrane localization regulation domain. Two closely spaced membrane hydrophobic helices tether the precursor SREBP in the ER membrane, where it forms a complex with the SREBP cleavage-activating protein (SCAP) (Sakai et al., 1997). ER localized SCAP interacts with a third ER membrane protein called INSIG, and the SCAP-INSIG association effectively anchors the precursor SREBP in the ER (Yang et al., 2002). When cellular lipid levels decline, or other conditions arise where increased nuclear SREBP levels are required (Jeon and Osborne, 2012), key signaling pathways decrease the SCAP-INSIG interaction. Then, the COPII trafficking system escorts the SCAP-SREBP complex to the Golgi apparatus where two resident proteases sequentially cleave the SREBP precursor, leaving the membrane anchor linked to the Golgi membrane and releasing the mature soluble SREBP transcription factor that is rapidly targeted to the nucleus (Sun et al., 2007).

INSIG proteins also interact directly with the ER membrane-localized HMG CoA reductase enzyme, which catalyzes a key early step in the endogenous synthesis pathway for Ch (Sever et al., 2003). INSIG directs HMG CoA reductase into a proteosomal degradation pathway so that, when new Ch synthesis is required, the INSIG-reductase interaction is disfavored, leading to a rapid increase in Ch synthesis. Thus, the connection between the rapid regulation of Ch biosynthesis through the stabilization of HMG CoA reductase with the slow-to-develop mechanism through SREBP-dependent activation of gene expression is coordinately integrated through protein-protein interactions with INSIGs.

Once in the nucleus, SREBPs activate the expression of many key genes for Ch synthesis and uptake, including those encoding the LDL receptor and HMG CoA reductase. Recent advances in genomic technologies have allowed the comprehensive interrogation of transcription factors at a genome-wide level, and, for SREBPs, these studies have definitively shown their direct roles in activating genes of lipid metabolism in concert with a preferred set of generic transcription factor partners (Reed et al., 2008; Seo et al., 2009; Seo et al., 2011). Additionally, these global studies have also provided evidence of a broader role for SREBPs in physiology and metabolism (Seo et al., 2011).

Genome-wide analyses of RNA transcription patterns have uncovered an extensive network of noncoding RNAs, including small microRNAs (miRNAs) (Bartel, 2004). miRNAs are processed from longer transcripts into mature ~22- to 24-nucleotide single-stranded RNAs. They are incorporated into RNA protein complexes and decrease messenger RNA (mRNA) stability and/or translation efficiency of target genes through base pair interactions between the miRNA and target mRNA. Recent estimates suggest there are approximately 1,000 miRNAs peppered throughout the mammalian genome, of which approximately half are encoded from their own transcriptional units, whereas the other half are embedded within the noncoding regions of primary host protein coding mRNAs (Small and Olson, 2011). Because the embedded miRNAs are processed from the host primary transcript, the expression of the miRNA is dependent on the same transcriptional regulatory mechanisms that govern the expression of the host gene. In contrast, the nonembedded miRNAs are uniquely expressed through regulatory interactions that specifically target their own promoters.

Recent studies have uncovered a pair of miRNAs, miR-33a and miR-33b, that are encoded within introns of the human *SREBF-2* and *SREBF-1* genes, respectively (Gerin et al., 2010; Horie et al., 2010; Marquart et al., 2010; Najafi-Shoushtari et al., 2010; Rayner et al., 2010). However, only miR-33a is conserved in the mouse genome. These two miRNAs have identical seed regions and, therefore, are predicted to inhibit expression from many of the same genes. One conserved miR-33 target gene encodes the ABCA1 transporter, which plays an important role in modulating intracellular Ch metabolism by effluxing free Ch to extracellular Ch carriers such as HDL. This pathway plays a key role in regulating reverse Ch transport from macrophages and is also part of the interactive mechanism for controlling intracellular Ch balance in many other cell types (Fernández-Hernando and Moore, 2011; Rottiers et al., 2011). Because the SREBF-2 gene is autoregulated, the increase in miR-33a and SREBP-2 provides two complementary mechanisms whereby increased SREBP-2 transcription increases intracellular Ch.

The SREBF-2 gene is autoregulated, and the magnitude of autoinduction is relatively mild at 2- to 3-fold, which is similar to the magnitude for miR-33a induction by sterol depletion in macrophages (Rayner et al., 2010). In contrast, other target genes show much more robust induction by SREBP (Horton et al., 2003; Yokoyama et al., 1993). Because intracellular Ch levels are tightly controlled (Goldstein and Brown, 1990), we reasoned that additional miRNAs might be involved in regulating intracellular Ch, possibly being more robustly activated by SREBPs than miR-33 and having unique target genes involved in the multistep SREBP regulatory pathway. In the current study, we performed a genome-wide analysis searching for miRNAs that are differentially expressed in the livers of mice fed a normal chow diet supplemented with excess Ch versus a chow diet supplemented with a combination of lovastatin plus ezetimibe (LE). Variations of this dietary regimen have been used for three decades to analyze the hepatic regulatory pathway for Ch metabolism (Bennett et al., 2008; Liscum et al., 1983; Seo et al., 2011; Sheng et al., 1995). The LE combination inhibits both endogenous Ch synthesis and dietary absorption of Ch, and, when combined with the Ch-supplemented group, the diets represent homeostatic extremes for hepatic Ch overload versus depletion.

We identified 30 differentially expressed miRNAs, 21 that were expressed at higher levels in the LE-supplemented group, and 9 that were more abundant in the Ch-fed sample. At the extreme, miR-182 was expressed at 80-fold higher levels in the LE versus the Ch group. miR-182, along with its two miRNA siblings, miR-96 and miR-183, is expressed from a unique primary transcript (Xu et al., 2007) at an miRNA locus on mouse chromosome 6, and we show that the promoter for this locus is a direct target for SREBP activation. We also demonstrate that miR-182 and miR-96 negatively regulate the expression of Fbxw7 and Insig-2, respectively; two proteins that are known to negatively influence the levels of nuclear SREBPs. Furthermore, we show that this regulatory pathway is conserved in human cells and that the direct manipulation of miR-182 and miR-96 expression leads to changes in nuclear SREBPs as well as alterations in endogenous lipid synthesis. Thus, we have uncovered a mechanism for the regulation of intracellular Ch metabolism mediated by the concerted action of a pair of miRNAs. Importantly, both miRNAs are expressed from the same SREBP-2-regulated miRNA transcription unit, and each miRNA targets a different protein in the multistep pathway that regulates SREBP action. Thus, this regulatory system is analogous to the classic operon mechanism for genetic regulation in bacterial systems where gene products that function together in a common biological pathway are coordinately expressed from the same primary transcript and from a single promoter that is regulated by the biological pathway associated with the operon (Jacob and Monod, 1961).

RESULTS

Molecular pathways that maintain hepatic Ch balance have been investigated in rodent models by combining dietary manipulations with statin supplementation for over three decades (Bennett et al., 2008; Liscum et al., 1983; Seo et al., 2011; Sheng et al., 1995). As novel methods, reagents, and molecular pathways have been developed or uncovered, the same basic dietary programs have been very useful in applying new principles to further understand the regulatory mechanism for Ch metabolism. For example, we recently uncovered an unexpected connection between autophagy and Ch regulation by combining a chromatin immunoprecipitation (ChIP) sequencing approach for the genome-wide localization of SREBP-2 in hepatic chromatin from mice fed a chow diet supplemented with LE to inhibit hepatic Ch synthesis and limit dietary absorption of Ch (Seo et al., 2011). In the current studies, we have used this dietary

comparison to analyze differences in expression for the individual members of the small miRNA family of noncoding transcripts.

Identification of 30 Ch-Regulated miRNAs in the Mouse Liver

We fed mice a regular chow diet supplemented with either excess Ch or the LE mixture and compared the expression of hepatic miRNAs from each group using a mouse tiling low-density PCR array (TLDA). A heat map for the data is presented in Figure S1 (available online) along with control measurements showing the LE-diet-induced expression of HMG CoA reductase mRNA and protein as well as the mature nuclear form of SREBP-2. The heat map emphasizes that there is a range in expression for individual miRNAs that includes some that are highly induced by the LE diet and some that were expressed at higher levels in the Ch-supplemented samples. In further analyzing the data, we focused on miRNAs that were expressed with a Ct value $\leq$ 35 with a differential expression of 2-fold or greater relative to the two treatment groups at $p \leq 0.05$ (Table 1). There were 30 miRNAs that met these stringent criteria, and they ranged from miR-182, which was expressed at 80-fold higher levels in the LE-treated livers, to miR-455, which was expressed at 25-fold higher levels in the Ch-fed group. The primers included with the TLDA kit do not accurately measure the expression of miR-33a, which is encoded within the *Srebf-2* host gene and is known to be autoregulated. However, this analysis did identify the complementary strand miRNA miR-33* as being increased 2- to 3-fold by LE supplementation.

miR-182 is expressed from a miRNA island locus on mouse chromosome 6 that also encodes miR-96 and miR-183. Interestingly, all three miRNAs are transcribed from a single promoter (Chien et al., 2011) and are part of the same primary transcript (Xu et al., 2007) (Figure 1, bottom). It was previously shown that the expression of this miRNA locus is activated during T helper cell clonal expansion (Stittrich et al., 2010) and light-dark transition in the retina (Krol et al., 2010). Interestingly, in both cases, miR-182 was more robustly expressed than the other two coexpressed miRNAs, which was similar to our results. To begin to evaluate the potential role for these miRNAs in regulating hepatic Ch metabolism, we analyzed the expression of each one separately with specific quantitative PCR (qPCR) analyses, and all three miRNA siblings were robustly induced by LE treatment (Figure 1A). We also measured miR-33 directly and confirmed that it was also induced by LE feeding as expected. In evaluating the TLDA data, the Ct values for miR-96 and miR-183 were below the 35-cycle cutoff in the Ch-fed sample and did not meet the stringent criteria we used to prepare the list in Table 1. The expression of these three miRNAs was also robustly increased in the livers of transgenic mice overexpressing SREBP-1a or SREBP-2, but not by SREBP-1c (Figure S2). These results suggest that the miRNA locus may be directly activated by SREBPs.

The miR-96/182/183 Locus Is Regulated by SREBP-2

On the basis of the above data, we reasoned that the promoter driving the expression of the miRNA locus might be directly regulated by SREBP-2. Computational methods have been used to predict putative miRNA promoters throughout the human genome by combining sequence analysis with epigenetic signatures and mapping short promoter-proximal RNA transcripts (Chien et al., 2011). This analysis predicted a putative promoter for the human miR-96/182/183 cluster. A sequence alignment with the corresponding region of the mouse genome revealed a high level of conservation between the two species (Figure S3A). It is noteworthy that there are conserved putative binding sites for SREBPs, as well as for other more generic transcription factors, such as Sp-1, NF-Y, and CREB and ATF, that have been shown to interact with SREBPs for efficient promoter activation (Osborne and Espenshade, 2009). Additionally, the expression of these human miRNAs were increased similarly to miR-33a in RNAs isolated from two different human hepatoma

Table 1. Hepatic miRNA Differential Expression Profiles from Mice Fed a Normal Chow Diet Supplemented with a Mixture of Lovastatin plus Ezetimibe versus Cholesterol

miRNA	Fold Change (LE/Ch)
182	81.6
470*	28.3
34b-3p	17.7
741	12.5
877	7.2
20b	6.2
297a*	5.7
19a	4.3
875-5p	3.6
33*	3.2
188-5p	3.2
467a*	3.0
195	2.9
877*	2.9
126-5p	2.8
130b	2.7
101a	2.3
339-3p	2.1
301b	2.1
331-3p	2.1
135a*	2.1
185	2.1
676	0.5
15a	.28
339-5p	.255
425	.23
221	.20
215	0.19
210	0.1
455	0.04

microRNA expression profiling for total RNAs pooled from six C57BL/6 mouse livers for each feeding condition. Expression was analyzed by TLDA profiling, as described in the Experimental Procedures. miRNA expression is displayed as the fold change from the lovastatin plus ezetimibe (LE) versus cholesterol (Ch). Only those miRNAs that were differentially expressed by $\geq$2-fold with a $p < 0.05$ with a Ct value $\leq$ 35 are shown.
See also Figure S1.

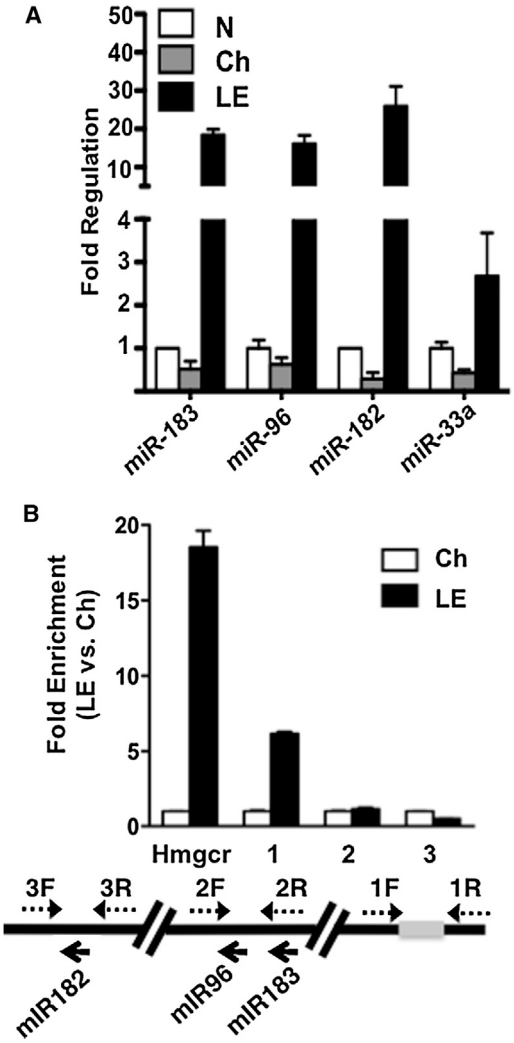

Figure 1. The miR-96/182/183 Locus Is Directly Regulated by SREBP-2

(A) qPCR analysis of miR-96, miR-182, and miR-183 in RNA from mice fed chow (N), chow supplemented with cholesterol (Ch), or chow supplemented with lovastatin plus ezetimibe (LE). Samples were normalized to sno202 RNA samples analyzed in parallel. Data are plotted relative to normalized values from the chow group set at 1.0.

(B) ChIP analysis for SREBP-2 binding in hepatic chromatin from Ch- versus LE-supplemented mice. The three regions in the miR-96/182/183 locus that were analyzed for SREBP-2 association are shown by the location of forward (F) and reverse (R) primer pairs 1, 2, or 3 used for the qPCR analysis as indicated. The thick gray box denotes the putative promoter region for the locus interrogated by primer pair 1, as discussed in the Results.

Data are represented as mean ± SEM. See also Figure S2.

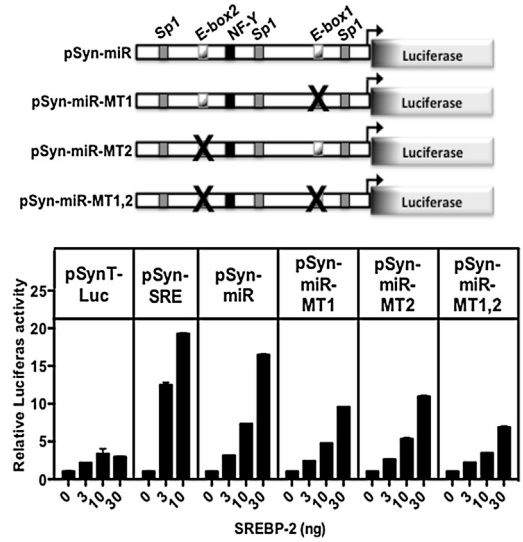

Figure 2. SREBP-2 Activates the miR-96/182/183 Promoter

The putative promoter region shown in gray at the bottom of Figure 1 was cloned upstream of luciferase in the control luciferase reporter, as shown and described in the Experimental Procedures. Key putative transcription-factor-binding sites that are conserved between mice and humans (Figure S3) are noted on the diagram of the sequence. Top, there are two E box motifs that are putative SREBP response elements, and point mutations were engineered into each separately or in combination, as noted by the X. Bottom, wild-type and the indicated mutant promoters were transfected into human embryonic kidney 293T cells along with increasing amounts of an SREBP-2 expression vector, as described in the Experimental Procedures. The negative and positive control promoters analyzed in parallel are shown as pSynTLuc and pSynSRELuc and are described elsewhere (Dooley et al., 1998). Luciferase activities were normalized to β-galactosidase that was expressed from an internal control cotransfected cytomegalovirus β-galactosidase plasmid.

Data are represented as mean ± SEM. See also Figure S3.

cells infected with an adenovirus expressing the mature form of SREBP-2 (Figure S3B). Thus, the human miR-96/182/183 locus is also most likely regulated directly by SREBPs.

This putative promoter region is schematically represented as a gray box in the diagram at the bottom of Figure 1. To determine whether the predicted SREBP sites are functional, we performed a ChIP study to evaluate SREBP-2 binding in chromatin prepared from the LE versus Ch samples. The results in Figure 1B demonstrate that SREBP-2 binds to this predicted promoter region in the LE chromatin (detected by primer pair 1F and 1R in Figure 1B), but not to the coding regions of the miRNA locus, which were analyzed as negative controls.

A cartoon diagram of the promoter region from Figure S3 is presented at the top of Figure 2 highlighting the E box sites, which are classic recognition elements for bHLH proteins, such as SREBPs, along with the predicted binding sites for the more generic transcription factors Sp1 and NF-Y, which are preferentially coenriched in SREBP target promoters (Seo et al., 2011). Next, we fused the putative promoter DNA from the mouse genome to luciferase and showed that luciferase expression was enhanced in a dose-dependent fashion by the cotransfection of an expression vector encoding the nuclear-targeted SREBP-2 protein (Figure 2, bottom). When the two predicted SREBP-binding E box elements were mutated, SREBP-2 activation was significantly reduced. Along with the ChIP studies, these results provide compelling evidence that the expression of the miR-96/182/183 locus is directly regulated by SREBP-2.

miR-96 and miR-182 Decrease the Expression of Insig-2 and Fbxw7, Two Proteins that Negatively Regulate Nuclear Levels of SREBP-2

miRNAs regulate gene expression through putative base-pair interactions with target mRNAs as part of the RNA-induced

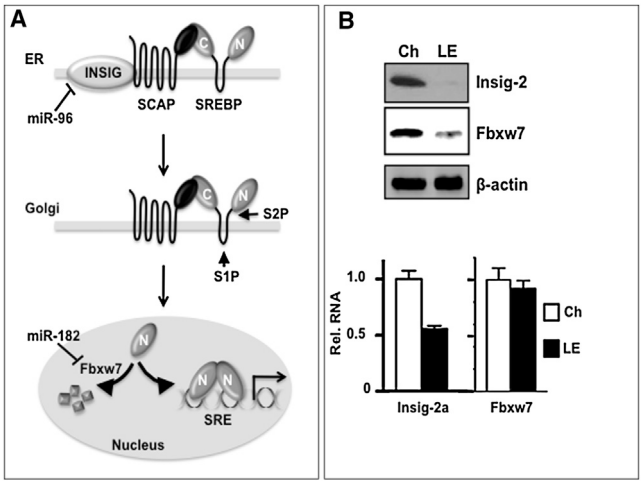

Figure 3. miR-96 and miR-182 Target Key Proteins of the SREBP Maturation Pathway

(A) A cartoon depicting key molecules and trafficking of the SREBP maturation pathway is presented along with the putative target genes for miR-96 and miR-182 as Insig and Fbxw7, respectively.

(B) Immunoblotting and qPCR analyses for Insig-2 and Fbxw7 in extracts from the livers of Ch- and LE-treated mice.

Data are represented as mean ± SEM. See also Figure S4 and Tables S1 and S2.

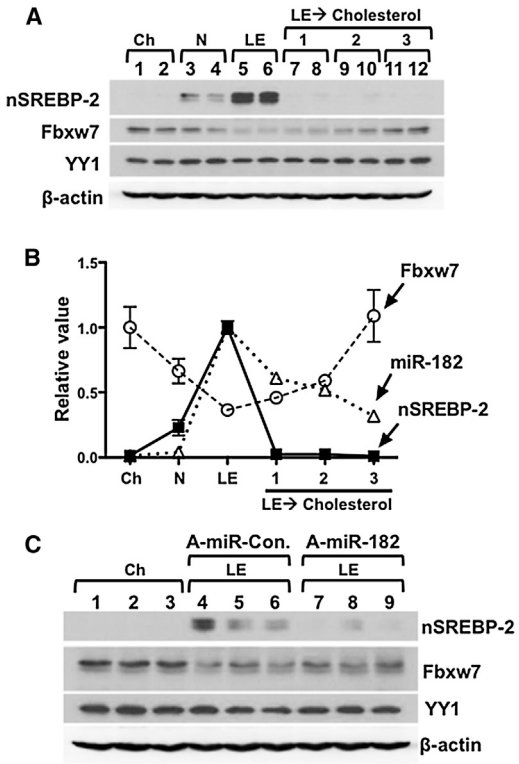

Figure 4. Coordinate and Reciprocal Regulation of nSREBP-2 with miR-182 or Fbxw7, Respectively

(A and B) Mice were fed chow (N) supplemented with Ch, LE, or LE followed by Ch for 1–3 days as indicated. Equal amounts of protein from two separate mice were analyzed for nSREBP-2, Fbxw7, and control proteins, as indicated by immunoblotting (A), and results were quantified and plotted as relative expression (B) along with the relative expression of miR-182 analyzed by qPCR.

(C) Hepatic protein from three individual mice was analyzed as in (A). Where indicated, a control anti-miRNA (A-miR-Con) or an anti-miRNA designed to target miR-182 (A-miR-182) were injected (30 mg/kg) on days 3, 4, and 5 of LE diet supplementation, and mice were sacrificed on day 7.

Data are represented ad mean ± SEM. See also Figure S5.

silencing complex (RISC) and reduce the expression of the encoded proteins by inhibiting translation and/or increasing mRNA degradation (Bartel, 2004). We hypothesized that, because the miR-96/182/183 locus is directly activated by SREBP-2, these miRNAs might target proteins involved in the SREBP regulatory pathway. Thus, the TargetScan program was used to identify putative target mRNAs for miR-96, miR-182, and miR-183, and this list was cross-matched for proteins that are known to be involved in the complex sterol-regulated SREBP proteolytic maturation pathway, which is partially diagrammed in Figure 3A. Lists of the highest-scoring putative gene targets predicted by TargetScan for miR-182 and miR-96 are shown in Table S1 and S2, respectively. This analysis predicted that genes encoding INSIG-2 and FBXW7 are putative targets of miR-96 and miR-182, respectively, across several mammalian species (Figures 3 and S4). In fact, there are two putative miR-182 sites within the FBXW7 3′ untranslated region (3′UTR). INSIG-2 is key for retaining the SCAP-SREBP-precursor complex in the ER (Yabe et al., 2002) (Figure 3A), and FBXW7 is the E3 ubiquitin ligase that targets nuclear SREBPs for proteasomal degradation (Sundqvist et al., 2005) (Figure 3A). Because INSIGs and FBXW7 both limit the accumulation of nuclear SREBPs, the elevated expression of miRNAs that target these proteins would be predicted to increase nuclear SREBP-2, which is a signature hepatic response of the LE dietary supplementation. To test this prediction, we measured Insig-2 and Fbxw7 mRNA and protein levels in extracts from Ch- or LE-treated mice. The results demonstrate that Insig-2 and Fbxw7 protein levels were both significantly lower in the LE- versus Ch-fed samples (Figure 3B). Interestingly, this was accompanied by a decrease in Insig-2 mRNA, but Fbxw7 mRNA was not significantly altered. These results are consistent with miR-96 and miR-182 targeting Insig-2 and Fbxw7, respectively.

Additional studies were focused on Fbxw7, given that the Ct value for miR-182 suggested that it was more highly expressed after LE treatment than miR-96 and miR-183 in the liver. We reasoned that, if miR-182 repression of Fbxw7 was crucial for increasing SREBP-2 levels in response to LE feeding, then the addition of Ch after LE induction would coordinately suppress SREBP-2 and miR-182 while reciprocally increasing the expression of Fbxw7 back to the level observed in control animals. The results in Figures 4A and 4B show that the increase in expression of both SREBP-2 and miR-182 in response to LE supplementation was significantly suppressed after 1 day of Ch supplementation. Additionally, the low levels of Fbxw7 protein observed after LE supplementation increased steadily as miR-182 levels declined over the course of 3 days of Ch feeding. We also measured the expression of SREBP-2 mRNA along with its embedded miRNA, miR-33a. As predicted, the expression of SREBP-2 and miR-33a were induced similarly by LE and suppressed in parallel by Ch addition (Figure S5).

To directly determine whether the increase in miR-182 following LE treatment contributes to the increased nuclear

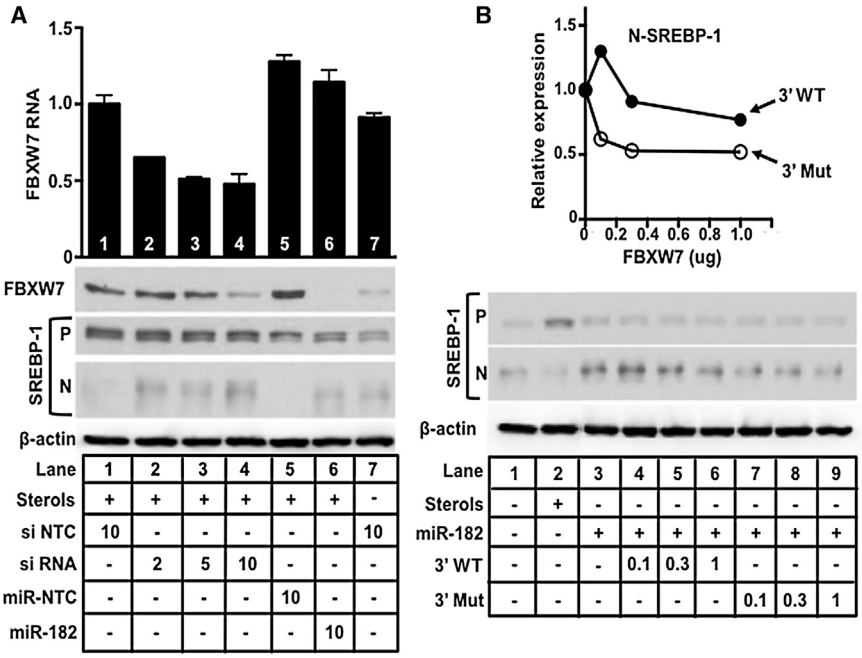

Figure 5. Regulation of SREBPs by the miR-182 Locus through FBXW7 Is Conserved in Human Cells

(A) HeLa cells were transfected with siRNA or pre-miRNAs as indicated (10 nM, Ambion) in antibiotic-free medium as described in Materials and Methods. After 24 hr, the dishes were switched to DMEM containing 5% lipoprotein-deficient serum, 12 μg/ml Ch, and 1 μg/ml 25-hydroxycholesterol and incubated for 24 hr at 37°C. Also shown are qPCR for FBXW7 and immunoblotting for FBXW7, SREBP-1, and β-actin.

(B) The full-length FBXW7 coding sequence was cloned downstream of the constitutive RPL10 promoter with the natural FBXW7 3′UTR intact. We also prepared a version where the two predicted miR-182 targeting sites were mutated to decrease the predicted complementarity. These constructs were transfected into HeLa cells in combination with miR-182 or controls and cultured as described in the Experimental Procedures and in the figure diagram. Quantitation from a scanned image of the immunoblot is presented at the top.

Data are represented as mean ± SD. See also Figure S6.

accumulation of SREBP-2, we treated mice with LE and injected them with an anti-miRNA designed to pair with and inactivate miR-182. The results show that anti-miR-182 treatment blunted the induction of SREBP-2 by LE treatment (Figures 4C and S6). The expression of some SREBP target genes, such as SREBP-2 itself, were also reduced (Figure S6), whereas others, such as Hmgcr, were minimally affected (Figure S6). This is consistent with many other observations that demonstrate that individual SREBP target genes are differentially affected by direct changes in SREBP levels (Osborne and Espenshade, 2009).

Fbxw7 protein levels were only minimally affected by the anti-miRNA-182 treatment (Figures 4C and S6), suggesting there are other miR-182 target genes involved in regulating nuclear SREBP levels. Mice were also injected with anti-miRNAs targeting either miR-96 or miR-183, and neither miRNA resulted in a decrease in nuclear SREBP-2 (Figure S6). Altogether, the results suggest that miR-182 plays a dominant role in the regulation of SREBP-2 under these conditions, which is consistent with its more robust induction relative to the other two miRNAs in response to the LE diet challenge.

miRNA Regulation of SREBPs through FBXW7 Is Conserved in Human Cells

To analyze the role of miR-182 in regulating human SREBPs through FBXW7, we compared the effects of direct small interfering RNA (siRNA) targeting of Fbxw7 to miR-182 on nuclear SREBP levels in HeLa cells (Figure 5A). Treatment of HeLa cells with siRNA targeting FBXW7 resulted in an increase in nuclear SREBP-1, and this was similar to the samples treated with pre-miR-182. The magnitude of the induction of nuclear SREBP-1 was similar to that obtained by sterol depletion, which is the classic treatment for inducing nuclear SREBP accumulation in cultured cells (Brown and Goldstein, 1986, 1999). Interestingly, although siRNA targeting resulted in parallel reduction in FBXW7 mRNA and protein, the pre-miR-182 treatment resulted in a decrease in FBXW7 protein without a change in RNA. This is consistent with the effects observed for the LE diet treatment on Fbxw7 levels in mice (Figure 3).

Increase in Nuclear SREBP-2 Mediated by miR-182 Transfection Is Reversed by the Reintroduction of Ectopic FBXW7 and Is Sensitive to the 3′UTR

To directly analyze the effects of miR-182 on FBXW7 protein expression, we transfected HeLa cells with an expression vector encoding the full-length SREBP-2 protein, including its carboxy-terminal membrane-targeting domain and a FLAG epitope tag at the amino terminus. Where indicated, cells were cotransfected with pre-miR-182, and, in order to restore FBXW7, an expression vector encoding FBXW7 (without its native 3′UTR) was added as shown in Figure S6A. In this study, the increase in nuclear SREBP-2 that resulted from pre-miR-182 addition was similar to that observed when cells were depleted of endogenous sterols. Importantly, the effect was reversed when the FBXW7 expression vector was also included, which was consistent with FBXW7 being the major target of miR-182 for the regulation of nuclear SREBP levels under these conditions.

To determine whether the effect of ectopic FBXW7 was sensitive to miR-182 targeting the predicted miR-182-binding sites in the FBXW7 3′UTR, we performed two experiments. First, we expressed FBXW7 protein from a constitutive mRNA that contains either its natural 3′UTR or a mutant version where both predicted miR-182-targeting sites (Figure S4) were changed to destroy complementarity (Figure 5B). We also showed that FBXW7 protein was expressed at similar levels from both constructs in transfected cells (Figure S6). When we cotransfected a pre-miR-182 along with the two FBXW7 expression constructs, only the one with the mutated miR-182-targeted sites was able to decrease the nuclear SREBP-1. In a separate experiment, we also inserted the wild-type and mutant FBXW7 mRNA 3′UTR regions downstream from the luciferase coding sequence

driven by a constitutive ribosomal protein gene 10 promoter (Figure S6). When these two luciferase expression constructs were transfected into mammalian cells, luciferase expressed from the FBXW7 construct containing the native FBXW7 3′UTR was suppressed by the addition of miR-182, whereas luciferase expressed from the 3′UTR mutant construct was not affected. We also performed a similar experiment to analyze miR-96 targeting of INSIG-2 (Figure S6). In this experiment, the reduction in luciferase expression in response to miR-96 cotransfection was abrogated when the bases complementary to the miRNA seed sequences in the corresponding 3′UTRs (Figure S4) were mutated (Figure S6). Altogether, the results from the cotransfection studies with the mutant 3′UTRs support our conclusions that miR-182 directly targets the FBXW7 3′UTR and that miR-96 directly targets the INSIG 2 3′UTR.

miR-96, miR-182, and miR-183 Regulate Lipid Synthesis through the Modulation of Nuclear SREBP Levels

The miR-96/182/183 locus is conserved in humans, and sequence alignment predicts that human INSIG-2 and FBXW7 are also targeted by the corresponding human miRNAs (Figure S4). To test this prediction, HeLa cells were cultured in the presence of sterols, where nuclear levels of SREBPs are low and cells were treated with individual pre-miRNAs corresponding to human miR-96, miR-182, miR-183, or the combination of all three pre-miRNAs (Figure 6A). Nuclear SREBP-1 was increased similarly by each individual miRNA or the combination. There was a similar increase in SREBP-2 nuclear accumulation, and SREBP target genes were stimulated in parallel with changes in nuclear SREBPs (Figure S7).

To determine whether the regulation of SREBP levels by this miRNA pathway had a significant physiologic impact on endogenous lipid synthesis, we measured the effects of the combination of all three pre-miRNAs on the synthetic rates for fatty acids and Ch in HeLa cells. The low level of endogenous lipid synthesis in sterol-treated HeLa cells was significantly enhanced by the pre-miRNA combination (Figure 6B).

DISCUSSION

In classic experiments dating to the middle of the last century, hepatic Ch synthesis was suppressed when animals were fed a diet supplemented with excess Ch (Gould, 1951; Langdon and Bloch, 1953). This first demonstration of end-product repression in a complex mammalian system in vivo predated most of the key experiments that defined the fundamental molecular mechanisms for nutrient sensing in bacteria (Monod et al., 1963). Since that time, mammalian Ch metabolism has been an experimentally rich and clinically relevant experimental system for understanding how the classic regulatory mechanisms for small-molecule sensing have evolved to maintain homeostasis in a complex and highly integrated multicellular eukaryotic environment (Brown and Goldstein, 2009).

Using an updated version of the original animal feeding protocol, we have uncovered a role for a coordinately expressed cluster of noncoding miRNAs in the pathway that maintains feedback control of intracellular lipid metabolism. In an unbiased screen, we noticed that levels of miR-96, miR-182, and miR-183 were dramatically increased in the livers of mice fed a chow diet

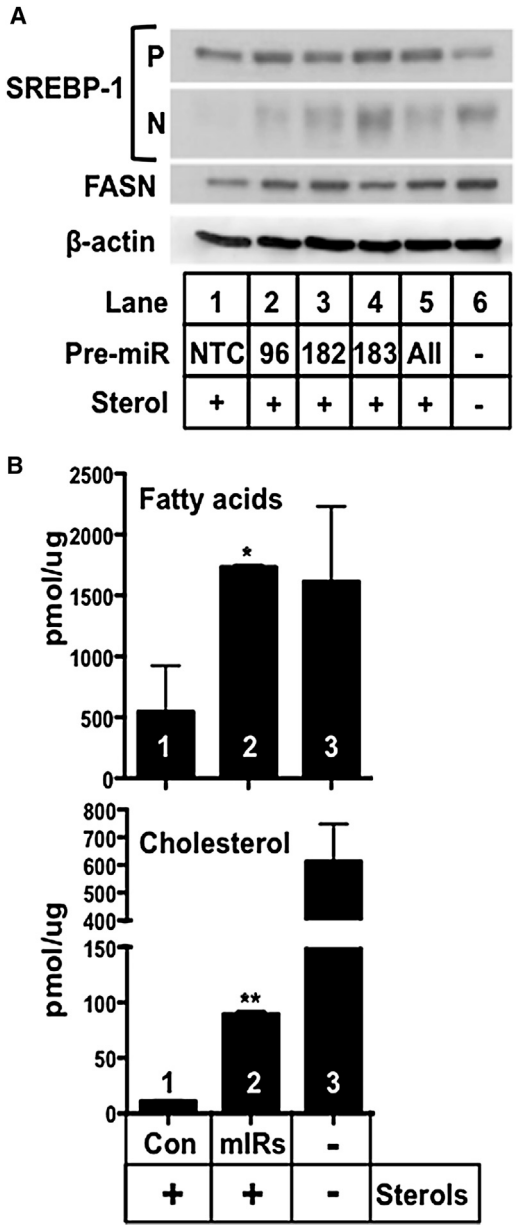

Figure 6. miRNA Regulation of SREBP Levels Is Accompanied by the Robust Induction of Lipid Biosynthesis

(A) HeLa cells were transfected with the indicated human pre-miRNAs alone or in combination (10 nM, Ambion), as indicated and cultured in antibiotic-free medium. After 24 hr, the dishes were switched to DMEM containing 5% lipoprotein-deficient serum with or without sterol mixture (12 μg/ml Ch and 1 μg/ml 25-hydroxycholesterol) and incubated for 24 hr at 37°C and harvested. Western blot analysis for the precursor (P) and nuclear (N) form of SREBP-1 was performed. Fatty acid synthase protein was also analyzed by immunoblotting (FASN), and β-actin was measured as a control.

(B) Companion dishes of HeLa cells were treated as in (A), and de novo synthesis of fatty acid and Ch were measured with [^{14}C] acetate incorporation. Either control miRNA (Con) or a mixture of all three specific miRNAs (miR-96, miR-182, and miR-183) were added together. The p values for differences relative to control were *$p = 0.035$ for fatty acids and **$p < 0.0001$ for Ch. Data are represented as mean ± SEM. See also Figure S7.

supplemented with LE relative to a group fed chow supplemented with excess Ch. These three conserved miRNAs are transcribed together in the same transcription unit to from a miRNA locus on mouse chromosome 6 and the homologous region from human chromosome 7 (Chien et al., 2011; Xu et al., 2007). Nuclear SREBP-2 levels increase dramatically by the LE feeding protocol, and the expression of this miRNA locus was also induced along with the known SREBP-2 transcriptional program driving lipid accumulation. We also showed that SREBP-2 binds to the promoter for the miRNA locus, providing a mechanism for the LE-dependent induction.

Additional studies demonstrated that the promoter driving the expression of the miRNA locus encoding miR-96/182/183 is directly activated by SREBP-2. We also show that miR-96 inhibits Insig-2, that miR-182 inhibits Fbxw7, and that both of these proteins have well-described roles in limiting the accumulation of nuclear SREBPs, as diagrammed in Figure 3A (Sundqvist et al., 2005; Yabe et al., 2002). Insig-2 reduces the proteolytic activation of the membrane-bound SREBP precursor, and Fbxw7 is the E3 ubiquitin ligase that targets nuclear SREBPs for turnover by the proteasome. In fact, the major effect of a hepatic knockout of Fbxw7 was an increase in nuclear SREBPs and hepatic lipid accumulation (Onoyama et al., 2011), which further emphasizes the importance of Fbxw7 in hepatic lipid accumulation and the SREBP pathway. Additionally, an FBXW7 siRNA titration experiment showed that a similar change in FBXW7 mediated by miR-182 resulted in an increase in nuclear SREBP levels in HeLa cells.

Treatment of HeLa cells with pre-miR-183 also increased nuclear SREBP-1, suggesting that miR-183 also targets a protein(s) involved in regulating SREBP levels. We were initially encouraged when a target scan predicted that miR-183 might target Insig-1 directly. However, we have been unable to confirm this by direct studies with pre-miR-183 and the INSIG-1 3′UTR reporter. Unfortunately, there were no other obvious SREBP-pathway-associated genes within the list of putative miR-183 candidates predicted by TargetScan (data not shown) or additional prediction programs. Our results strongly suggest that miR-183 targets a key gene that regulates nuclear SREBP levels; however, its identification will require the development of more robust and accurate methods for identifying miRNA target genes. Because miRNAs often target several genes in the same pathway, it is also possible that future studies will identify additional relevant target genes of miR-96 and miR-182 as well.

The miRNA regulatory pathway described here is conserved from mice to humans, and we show that the introduction of the corresponding pre-miRNAs into human cells increases nuclear levels of both SREBP-1 and SREBP-2. Importantly, this is accompanied by an increase in the rates of synthesis for fatty acids and Ch, which are major physiological outcomes for increased SREBP activity. It is noteworthy that the increase in lipid synthesis occurs in cells cultured in the presence of excess sterols, indicating that this miRNA pathway can significantly affect lipid metabolism in the absence of other signals that increase SREBP activity in response to low intracellular sterol conditions. Even though the addition of ectopic miRNAs can drive significant SREBP accumulation in transfected cells, this miRNA pathway represents only a portion of the overall multifaceted mechanism for regulating SREBP levels in response to physiologic cues. This is evident from the experiment where Ch was added to the diets of mice that were pretreated with LE to induce SREBP-2. In this experiment, SREBP-2 protein levels decline rapidly and dramatically, whereas the levels of miR-182 decline more slowly over time.

miR-182 has also been implicated in oncogenesis, and anti-miRNA targeting of miR-182 decreases hepatic metastasis in a mouse melanoma model (Huynh et al., 2011). Although comparative microarray analyses showed several putative miR-182 target genes were altered by the anti-miRNA targeting in this study, the identity of key oncogenic targets were not clearly established. On the basis of our studies and the known role of Fbxw7 in regulating the turnover of cyclins (Koepp et al., 2001) and oncogenes such as c-Myc and c-Jun (Nateri et al., 2004; Yada et al., 2004), it is possible that Fbxw7 is an important target in this liver metastasis model as well.

The hepatic induction of miR-182 by LE treatment was significantly more robust than for miR-96 and miR-183. A similar differential accumulation of miR-182 was also observed when the locus was activated during the clonal expansion of T helper cells (Stittrich et al., 2010). The reason for the differential accumulation of miR-182 relative to the others is not clear because all three are processed from the same initial transcript. However, individual miRNAs are assembled into an active RISC after a multistep processing and assembly pathway, and the mechanistic details are not fully understood (Bartel, 2004, 2009). Thus, it is likely that the differential accumulation and loading of specific miRNAs into the RISC is related to differences in the efficiency of pre-miRNA processing and differential complex assembly.

The concentration of miR-182 decreased by approximately 50% from its peak value in the LE treatment group after 1 day of Ch supplementation, and it declined more over the course of the experiment. Thus, hepatic miR-182 levels respond more rapidly than miRNAs in general, which have been reported to be quite stable and to have an average half-life of approximately 5 days (Gantier et al., 2011). miR-182 levels also change quickly during the light-dark transition in the retina (Krol et al., 2010). Thus, relatively rapid changes in miR-182 levels are compatible with a significant role in more dynamic metabolic control.

miRNA regulation often results in modest decreases in target protein expression. However, singular miRNAs are known to target several proteins in a common pathway, so, even though individual changes are modest, the overall effect on pathway flux can be quite significant (Small and Olson, 2011). Our studies reveal another mode of miRNA regulation of a biological pathway where two separate miRNAs that are encoded from a common RNA transcript (Chien et al., 2011; Xu et al., 2007) target different steps in a pathway that regulates a transcription factor that controls expression from the corresponding miRNA promoter. In this way, our study reveals a regulatory loop whereby SREBP-2 controls expression from a genetic locus that produces miRNAs that regulate SREBP activity (Figure S7C). This mechanism is reminiscent of the classic ''operon'' paradigm for coordinate regulation of biological processes in bacterial systems where gene products that function together in a common pathway are coordinately expressed from one primary transcript and downstream from one promoter that is regulated by the biological process associated with the gene products encoded by the operon

(Jacob and Monod, 1961; Monod et al., 1965). In bacteria, end-product repression of amino acid operons occurs through a transcriptional regulatory protein that is also subject to autoregulation. It is interesting that this common feature is also shared with the miRNA-SREBP-2 regulatory circuit we describe here (Figure S7C). Because a prominent feature of the operon mechanism of genetic control is a polycistronic mRNA, it was unknown whether this mechanism was conserved in eukaryotic organisms where mRNAs are monocistronic and transcription and translation occur in separate cellular compartments. However, because miRNAs are encoded in polycistronic units and the RNAs function as the active gene products, it was formally possible that miRNA operons might exist in eukaryotic organisms. The SREBP-regulated miRNA operon described here constitutes an example of a true eukaryotic operon.

Overall, this study has uncovered a unique role for miRNA-dependent regulation of intracellular lipid metabolism that is integrated with the INSIG-SCAP pathway for controlling nuclear SREBP levels. Several other miRNAs were differentially expressed in the TLDA array profile from LE versus Ch feeding groups. Recent studies indicate that SREBPs link lipid metabolism with additional physiologic processes (Jeon and Osborne, 2012), and it is likely that future studies will reveal new roles for these other miRNAs and, perhaps, additional target genes of the miR-96/182/183 locus in the integrated processes controlled by SREBP action.

EXPERIMENTAL PROCEDURES

Animals

All animal experiments were performed in accordance with accepted standards of animal welfare and with permission of the Sanford-Burnham Medical Research Institute at Lake Nona International Animal Care and Use Committee (protocol 2012-88). We obtained 6-week-old male C57BL/6 mice from the Jackson Laboratory and maintained them on a chow diet for 1 week with a 12 hr light, 12 hr dark cycle for acclimatization.

For miRNA expression profiling, mice were separated into two groups of six animals per group and treated as described by Seo et al. (2011). In brief, one group was fed with normal chow supplemented with Ch (1% w/w) for 10 days, and another group was fed with chow supplemented with a mixture of lovastatin (100 mg lovastatin [2.5 tablet equivalents]/100 g chow, w/w; Mylan) and ezetimibe (from Schering-Plough Pharmaceuticals; 21 mg ezetimibe [2.1 tablet equivalents]/100 g chow, w/w) for 7 days. All mice were sacrificed at 8 a.m. (at the end of the dark cycle) via CO_2 asphyxiation followed by cervical dislocation. This basic feeding regimen was used in all experiments, and specific variations are described in the appropriate figure legends.

For the anti-miRNA experiment, mice were fed Ch or LE as above, and control or experimental anti-miRNA oligonucleotides were dissolved in 1 × PBS and intraperitoneal injected at 30 mg/kg on days 4, 5, and 6 at 8 a.m. (end of the dark cycle). Mice were sacrificed on day 7 at the end of the dark cycle.

RNA Isolation, qRT-PCR, and miRNA Expression Profiling and Validation

Total RNA was isolated from mouse liver and cultured cells with a mirVana miRNA Isolation Kit (Ambion). Primer sequences used in this study are provided in Figure S7D. mRNA levels were normalized for the expression of mouse ribosomal protein L32 and human glyceraldehyde 3-phosphate dehydrogenase mRNA as a control and calculated by the comparative threshold cycle method. miRNA expression profiling was carried out with the TaqMan Rodent Array MicroRNA Card Set v2.0 (Applied Biosystems) in triplicate at the Sanford-Burnham Genomics Core facility. Then, differential expression was assessed with the Partek Genomics Suite (Partek). Then, expression levels for miRNAs were quantified with a TaqMan MicroRNA Assay kit (Applied Biosystems) with a CFX96 Real-Time PCR Detection System (Bio-Rad). miRNA expression levels were normalized to sno202 (for mouse) and RNU48 (for human) expression.

Cell Culture and Small RNA Transfection

HeLa cells were maintained in Dulbecco's modified Eagle's medium (DMEM) supplemented with 10% heat-inactivated fetal bovine serum (FBS) and antibiotics in an atmosphere of 5% CO_2 at 37°C. HeLa cells were transfected with 10 nM pre-miRNAs (Ambion) with Lipofectamine RNAiMAX Reagent (Invitrogen) or FBXW7 siRNA (Dharmacon) using a Dharmafect 1 reagent. Manipulations were performed according to the manufacturer's instructions, and cells were cultured in DMEM with 10% FBS without antibiotics. HeLa cells were switched to DMEM containing 5% lipoprotein-deficient serum (LPDS, Sigma-Aldrich) and sterols (12 μg/ml Ch, 1 μg/ml 25-hydroxycholesterol) 24 hr after transfection. Cells were harvested 24 hr later. Where indicated, plasmids encoding the full-length human SREBP-2 with three copies of the FLAG epitope (a gift from J. Rutter) or human FBXW7 with a GST tag (Sundqvist et al., 2005) were included in the transfection.

ChIP Assay

Chromatin preparations for ChIP assays with mouse livers were performed as previously described (Bennett et al., 2008; Seo et al., 2009). For gene-specific ChIP, qPCR analysis of SREBP-2 binding to specific gene promoters was performed in triplicate with a standard dilution curve of the input DNA performed in parallel, and enrichment was measured by SYBR green incorporation with the use of a CFX-96 Real-Time PCR Detection System. Analyses were performed by the standard curve method, and values were normalized relative to a nontarget control region from the ribosomal L32 gene. The qPCR oligonucleotide pairs for the mouse promoters are provided in Figure S7.

De Novo Lipid Biosynthesis Assay

HeLa cells were transfected with pre-miRNAs as described above. Cells were switched to DMEM containing 5% LPDS with or without sterols for 24 hr. Cells were incubated in DMEM containing 5% LPDS 24 hr later, with or without sterols, plus 0.5 mM sodium [^{14}C]-acetate for the indicated times up to 3 hr. The cells were harvested by scraping into 0.5 ml 0.1 N NaOH followed by 0.5 ml distilled water, and 100 μl of the cell lysate was used to determine cellular protein content with a Pierce BCA Protein Assay Kit (Thermo Scientific). The contents of [^{14}C]-labeled Ch and [^{14}C]-labeled fatty acids were extracted from the remainder of the lysates as previously described (Horton et al., 1999) and spotted onto plastic-backed silica gel thin-layer chromatography (TLC) plates (Macherey-Nagel). TLC plates were resolved in chloroform or a heptane:diethyl ether:acetic acid (90:30:1) mixture (fatty acids) and stained with iodine vapor. The TLC spots were excised and transferred to scintillation vials containing 10 ml Ultima Gold XR scintillation fluid (PerkinElmer) for radioactive counting of [^{14}C] and [^{3}H]. The rate of incorporation for the 3 hr time course was linear under all assay conditions, indicating that the endogenous acetate pool was unaffected by the sterol manipulation (data not shown). All data for each sample were normalized to starting protein concentration and extraction efficiency with the internal [^{3}H]-chloroform and [^{3}H]-oleic acid standards. Data were reported as [^{14}C]-acetate incorporation per unit mass of protein (nmol/mg protein).

Statistics

The data are presented as mean ± SEM or mean ± SD, as detailed in the figure legends. Differences between the means of the individual groups were assessed by one-way ANOVA with a Dunnet's multiple comparison test and a Student's t test. Differences were considered significant at $p < 0.05$. The statistical software package Prism 5.0 (GraphPad) was used for these analyses.

SUPPLEMENTAL INFORMATION

Supplemental Information contains Supplemental Experimental Procedures, four figures, and two tables can be found with this article online at http://dx.doi.org/10.1016/j.cmet.2013.06.010.

ACKNOWLEDGMENTS

This work was supported, in part, by a grant from the NHLBI/NIH (HL48044). Y.-A.M. was supported by HL020948-36. We thank R. Debose-Boyd for

supplying the HMG CoA reductase and Insig-2 antibodies, J. Rutter for the FLAG-tagged SREBP-2 vector, and J. Ericsson for the GST-tagged FBXW7 expression plasmid.

Received: November 26, 2012
Revised: March 13, 2013
Accepted: June 12, 2013
Published: July 2, 2013

REFERENCES

Bartel, D.P. (2004). MicroRNAs: genomics, biogenesis, mechanism, and function. Cell *116*, 281–297.

Bartel, D.P. (2009). MicroRNAs: target recognition and regulatory functions. Cell *136*, 215–233.

Bennett, M.K., Seo, Y.K., Datta, S., Shin, D.J., and Osborne, T.F. (2008). Selective binding of sterol regulatory element-binding protein isoforms and co-regulatory proteins to promoters for lipid metabolic genes in liver. J. Biol. Chem. *283*, 15628–15637.

Brown, M.S., and Goldstein, J.L. (1986). A receptor-mediated pathway for cholesterol homeostasis. Science *232*, 34–47.

Brown, M.S., and Goldstein, J.L. (1999). A proteolytic pathway that controls the cholesterol content of membranes, cells, and blood. Proc. Natl. Acad. Sci. USA *96*, 11041–11048.

Brown, M.S., and Goldstein, J.L. (2009). Cholesterol feedback: from Schoenheimer's bottle to Scap's MELADL. J. Lipid Res. Suppl. *50*, S15–S27.

Chien, C.H., Sun, Y.M., Chang, W.C., Chiang-Hsieh, P.Y., Lee, T.Y., Tsai, W.C., Horng, J.T., Tsou, A.P., and Huang, H.D. (2011). Identifying transcriptional start sites of human microRNAs based on high-throughput sequencing data. Nucleic Acids Res. *39*, 9345–9356.

Dooley, K.A., Millinder, S., and Osborne, T.F. (1998). Sterol regulation of 3-hydroxy-3-methylglutaryl-coenzyme A synthase gene through a direct interaction between sterol regulatory element binding protein and the trimeric CCAAT-binding factor/nuclear factor Y. J. Biol. Chem. *273*, 1349–1356.

Fernández-Hernando, C., and Moore, K.J. (2011). MicroRNA modulation of cholesterol homeostasis. Arterioscler. Thromb. Vasc. Biol. *31*, 2378–2382.

Gantier, M.P., McCoy, C.E., Rusinova, I., Saulep, D., Wang, D., Xu, D., Irving, A.T., Behlke, M.A., Hertzog, P.J., Mackay, F., and Williams, B.R. (2011). Analysis of microRNA turnover in mammalian cells following Dicer1 ablation. Nucleic Acids Res. *39*, 5692–5703.

Gerin, I., Clerbaux, L.A., Haumont, O., Lanthier, N., Das, A.K., Burant, C.F., Leclercq, I.A., MacDougald, O.A., and Bommer, G.T. (2010). Expression of miR-33 from an SREBP2 intron inhibits cholesterol export and fatty acid oxidation. J. Biol. Chem. *285*, 33652–33661.

Goldstein, J.L., and Brown, M.S. (1990). Regulation of the mevalonate pathway. Nature *343*, 425–430.

Gould, R.G. (1951). Lipid metabolism and atherosclerosis. Am. J. Med. *11*, 209–227.

Horie, T., Ono, K., Horiguchi, M., Nishi, H., Nakamura, T., Nagao, K., Kinoshita, M., Kuwabara, Y., Marusawa, H., Iwanaga, Y., et al. (2010). MicroRNA-33 encoded by an intron of sterol regulatory element-binding protein 2 (Srebp2) regulates HDL in vivo. Proc. Natl. Acad. Sci. USA *107*, 17321–17326.

Horton, J.D., Shimano, H., Hamilton, R.L., Brown, M.S., and Goldstein, J.L. (1999). Disruption of LDL receptor gene in transgenic SREBP-1a mice unmasks hyperlipidemia resulting from production of lipid-rich VLDL. J. Clin. Invest. *103*, 1067–1076.

Horton, J.D., Shah, N.A., Warrington, J.A., Anderson, N.N., Park, S.W., Brown, M.S., and Goldstein, J.L. (2003). Combined analysis of oligonucleotide microarray data from transgenic and knockout mice identifies direct SREBP target genes. Proc. Natl. Acad. Sci. USA *100*, 12027–12032.

Huynh, C., Segura, M.F., Gaziel-Sovran, A., Menendez, S., Darvishian, F., Chiriboga, L., Levin, B., Meruelo, D., Osman, I., Zavadil, J., et al. (2011). Efficient in vivo microRNA targeting of liver metastasis. Oncogene *30*, 1481–1488.

Jacob, F., and Monod, J. (1961). Genetic regulatory mechanisms in the synthesis of proteins. J. Mol. Biol. *3*, 318–356.

Jeon, T.I., and Osborne, T.F. (2012). SREBPs: metabolic integrators in physiology and metabolism. Trends Endocrinol. Metab. *23*, 65–72.

Koepp, D.M., Schaefer, L.K., Ye, X., Keyomarsi, K., Chu, C., Harper, J.W., and Elledge, S.J. (2001). Phosphorylation-dependent ubiquitination of cyclin E by the SCFFbw7 ubiquitin ligase. Science *294*, 173–177.

Krol, J., Busskamp, V., Markiewicz, I., Stadler, M.B., Ribi, S., Richter, J., Duebel, J., Bicker, S., Fehling, H.J., Schübeler, D., et al. (2010). Characterizing light-regulated retinal microRNAs reveals rapid turnover as a common property of neuronal microRNAs. Cell *141*, 618–631.

Langdon, R.G., and Bloch, K. (1953). The effect of some dietary additions on the synthesis of cholesterol from acetate in vitro. J. Biol. Chem. *202*, 77–81.

Liscum, L., Luskey, K.L., Chin, D.J., Ho, Y.K., Goldstein, J.L., and Brown, M.S. (1983). Regulation of 3-hydroxy-3-methylglutaryl coenzyme A reductase and its mRNA in rat liver as studied with a monoclonal antibody and a cDNA probe. J. Biol. Chem. *258*, 8450–8455.

Marquart, T.J., Allen, R.M., Ory, D.S., and Baldán, A. (2010). miR-33 links SREBP-2 induction to repression of sterol transporters. Proc. Natl. Acad. Sci. USA *107*, 12228–12232.

Monod, J., Changeux, J.P., and Jacob, F. (1963). Allosteric proteins and cellular control systems. J. Mol. Biol. *6*, 306–329.

Monod, J., Wyman, J., and Changeux, J.P. (1965). On the Nature of Allosteric Transitions: A Plausible Model. J. Mol. Biol. *12*, 88–118.

Najafi-Shoushtari, S.H., Kristo, F., Li, Y., Shioda, T., Cohen, D.E., Gerszten, R.E., and Näär, A.M. (2010). MicroRNA-33 and the SREBP host genes cooperate to control cholesterol homeostasis. Science *328*, 1566–1569.

Nateri, A.S., Riera-Sans, L., Da Costa, C., and Behrens, A. (2004). The ubiquitin ligase SCFFbw7 antagonizes apoptotic JNK signaling. Science *303*, 1374–1378.

Onoyama, I., Suzuki, A., Matsumoto, A., Tomita, K., Katagiri, H., Oike, Y., Nakayama, K., and Nakayama, K.I. (2011). Fbxw7 regulates lipid metabolism and cell fate decisions in the mouse liver. J. Clin. Invest. *121*, 342–354.

Osborne, T.F., and Espenshade, P.J. (2009). Evolutionary conservation and adaptation in the mechanism that regulates SREBP action: what a long, strange tRIP it's been. Genes Dev. *23*, 2578–2591.

Rayner, K.J., Suárez, Y., Dávalos, A., Parathath, S., Fitzgerald, M.L., Tamehiro, N., Fisher, E.A., Moore, K.J., and Fernández-Hernando, C. (2010). MiR-33 contributes to the regulation of cholesterol homeostasis. Science *328*, 1570–1573.

Reed, B.D., Charos, A.E., Szekely, A.M., Weissman, S.M., and Snyder, M. (2008). Genome-wide occupancy of SREBP1 and its partners NFY and SP1 reveals novel functional roles and combinatorial regulation of distinct classes of genes. PLoS Genet. *4*, e1000133.

Rottiers, V., Najafi-Shoushtari, S.H., Kristo, F., Gurumurthy, S., Zhong, L., Li, Y., Cohen, D.E., Gerszten, R.E., Bardeesy, N., Mostoslavsky, R., and Näär, A.M. (2011). MicroRNAs in metabolism and metabolic diseases. Cold Spring Harb. Symp. Quant. Biol. *76*, 225–233.

Sakai, J., Nohturfft, A., Cheng, D., Ho, Y.K., Brown, M.S., and Goldstein, J.L. (1997). Identification of complexes between the COOH-terminal domains of sterol regulatory element-binding proteins (SREBPs) and SREBP cleavage-activating protein. J. Biol. Chem. *272*, 20213–20221.

Seo, Y.K., Chong, H.K., Infante, A.M., Im, S.S., Xie, X., and Osborne, T.F. (2009). Genome-wide analysis of SREBP-1 binding in mouse liver chromatin reveals a preference for promoter proximal binding to a new motif. Proc. Natl. Acad. Sci. USA *106*, 13765–13769.

Seo, Y.K., Jeon, T.I., Chong, H.K., Biesinger, J., Xie, X., and Osborne, T.F. (2011). Genome-wide localization of SREBP-2 in hepatic chromatin predicts a role in autophagy. Cell Metab. *13*, 367–375.

Sever, N., Yang, T., Brown, M.S., Goldstein, J.L., and DeBose-Boyd, R.A. (2003). Accelerated degradation of HMG CoA reductase mediated by binding of insig-1 to its sterol-sensing domain. Mol. Cell *11*, 25–33.

Sheng, Z., Otani, H., Brown, M.S., and Goldstein, J.L. (1995). Independent regulation of sterol regulatory element-binding proteins 1 and 2 in hamster liver. Proc. Natl. Acad. Sci. USA *92*, 935–938.

Small, E.M., and Olson, E.N. (2011). Pervasive roles of microRNAs in cardiovascular biology. Nature *469*, 336–342.

Stittrich, A.B., Haftmann, C., Sgouroudis, E., Kühl, A.A., Hegazy, A.N., Panse, I., Riedel, R., Flossdorf, M., Dong, J., Fuhrmann, F., et al. (2010). The microRNA miR-182 is induced by IL-2 and promotes clonal expansion of activated helper T lymphocytes. Nat. Immunol. *11*, 1057–1062.

Sun, L.P., Seemann, J., Goldstein, J.L., and Brown, M.S. (2007). Sterol-regulated transport of SREBPs from endoplasmic reticulum to Golgi: Insig renders sorting signal in Scap inaccessible to COPII proteins. Proc. Natl. Acad. Sci. USA *104*, 6519–6526.

Sundqvist, A., Bengoechea-Alonso, M.T., Ye, X., Lukiyanchuk, V., Jin, J., Harper, J.W., and Ericsson, J. (2005). Control of lipid metabolism by phosphorylation-dependent degradation of the SREBP family of transcription factors by SCF(Fbw7). Cell Metab. *1*, 379–391.

Xu, S., Witmer, P.D., Lumayag, S., Kovacs, B., and Valle, D. (2007). MicroRNA (miRNA) transcriptome of mouse retina and identification of a sensory organ-specific miRNA cluster. J. Biol. Chem. *282*, 25053–25066.

Yabe, D., Brown, M.S., and Goldstein, J.L. (2002). Insig-2, a second endoplasmic reticulum protein that binds SCAP and blocks export of sterol regulatory element-binding proteins. Proc. Natl. Acad. Sci. USA *99*, 12753–12758.

Yada, M., Hatakeyama, S., Kamura, T., Nishiyama, M., Tsunematsu, R., Imaki, H., Ishida, N., Okumura, F., Nakayama, K., and Nakayama, K.I. (2004). Phosphorylation-dependent degradation of c-Myc is mediated by the F-box protein Fbw7. EMBO J. *23*, 2116–2125.

Yang, T., Espenshade, P.J., Wright, M.E., Yabe, D., Gong, Y., Aebersold, R., Goldstein, J.L., and Brown, M.S. (2002). Crucial step in cholesterol homeostasis: sterols promote binding of SCAP to INSIG-1, a membrane protein that facilitates retention of SREBPs in ER. Cell *110*, 489–500.

Yokoyama, C., Wang, X., Briggs, M.R., Admon, A., Wu, J., Hua, X., Goldstein, J.L., and Brown, M.S. (1993). SREBP-1, a basic-helix-loop-helix-zipper protein that controls transcription of the low density receptor gene. Cell *75*, 185–197.